고성능 히스테리 제어를 이용한 고전압 DC 전력시스템을 위한 Voltage Bus Conditioner

論 文
56P-2-4

A Voltage Bus Conditioner for a High Voltage DC Power Distribution System using High Performance Hysteresis Control

羅 在 斗†
(Jae-Du La)

Abstract - More and All-Electric Aircraft (AEA) carry many loads with varied functions. In particular, there may be large pulsed loads with short duty ratio, which can affect the normal operation of other loads. In this paper, a bi-directional converter with inductive storage is used as a voltage bus conditioner (VBC) to mitigate voltage transients on the bus. In addition, the constant frequency hysteresis control technique for a VBC is presented. A simple and fast prediction of the hysteresis band-width is implemented by the phase-lock loop control, keeping constant switching frequency. This technique offers the excellent dynamic response in load or parameter variation. The control performance is illustrated by simulated results with the SABER package. The proposed hysteresis control results in the shortest and the smallest excursions.

Key Words : Voltage bus conditioner, More and all-electric aircraft, Distributed power system, Hysteresis control

1. Introduction

"Distributed Power Systems" (DPSs) has been widely used various industrial/military applications such as spacecraft, aircraft, telecommunications, autonomous production lines, and defence electronic power systems. DPSs offer many advantages to power system designers: high power capability, high efficiency, reliability, modularity, redundancy, expandability, and reduced development cost [1-2]. In addition, the "More and All-Electric" concept, in conjunction with DPS, has been found in land and sea-based vehicles such as cars, tanks and ships [3-5]. In these applications power availability and power density are of paramount importance, and the developments appear to be more advanced and mature than those in the aerospace industry. The concept of AEA was developed in the early 80s [6]. In a more and all-electric aircraft (AEA), the present systems and assemblies, such as hydraulic and pneumatic actuators, are substituted with electrical actuators. Design studies [7-9] have shown that implementing AEA will result in significant weight savings and improved reliability. Other benefits are associated with the increased safety and reduced cost of ownership of the aircraft.

In an AEA with high voltage DC distribution power system, DC bus instability due to system interaction is one of the greatest concerns. An aircraft power system is made up of smaller power subsystems. Usually these smaller subsystems are designed individually, i.e. the design of each subsystem is only based on the stability requirement for its stand-alone operation. As a result, after system integration, the interaction between subsystems may cause performance degradation, and even system instability [10]. For example, a lot of loads in an AEA perform various functions, which are reflected in the type of load they present to the distribution and generation part of the electrical power distribution. Of particular concern are large pulse loads with short duty ratio, such as weapons and radar systems, as well as flight actuators. The resulting transients on the supplying voltage bus inevitably influence the rest of the loads and may affect their normal operation [11].

In an AEA power distribution system, DC bus instability mainly may result from the negative impedance due to the constant power loads, pulsed loads, system transients and so on. Thus, a power conditioner may be used to mitigate the voltage transients on the bus. "Voltage Bus Conditioners" (VBCs) [17] are power electronic converters that dampen the voltage transients on the bus. They achieve this by transiently injecting current into the bus,

† 교신저자, 正會員 : The University of Birmingham, 博士課程
E-mail : jxl399@bham.ac.uk
接受日字 : 2007年 3月 16日
最終完了 : 2007年 5月 4日

compensating for the finite impedances of the feeder and any filter placed across the generator. These VBCs can be divided into two types: voltage-storage and current-storage. One of the drawbacks of the voltage-storage VBC is that it inherently does not fully utilize the storage capacitor energy. The drawback of the current-storage VBC is large power losses of the storage inductor, however this can be overcome with the use of cryogenic power electronics and superconducting coils. Therefore, the current storage VBC will be an attractive solution for all future electric aircraft power system.

The choice and implementation of the controller for a VBC is very important for the achievement of a satisfactory performance level. Hysteresis control (in effect a type of "Sliding Mode Control" (SMC)) is one of many excellent controllers used widely in power electronic converter applications [12-14]. This control technique has the advantage of not only being simple, robust and stable regardless of load condition, but also having a very good transient response and inherent peak limiting. However, the main disadvantage is that the switching frequency varies significantly with line and load variation. This results in the load current harmonic ripple and irregular converter operation. Alternatively, an effective control technique to eliminate these inconveniences is hysteresis control with constant switching frequency (with variable hysteresis band) [15-16]. The implementation of adapting hysteresis with a constant switching frequency could be easily implemented by "Phase Lock Loop" (PLL). In this paper, a current-storage VBC using constant frequency hysteresis control is used.

2. Converter Operation and Design

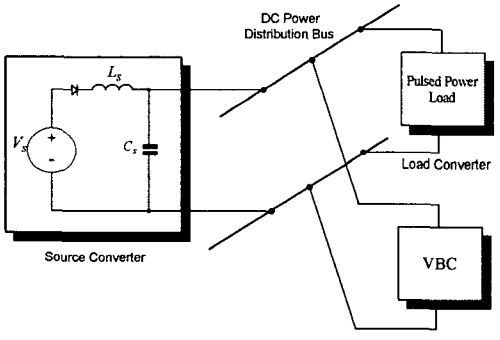

Fig. 1 A DC distributed power system

Fig. 1 is a simple DC distributed power system configuration, which is used to investigate the operation and the performance of the bi-directional converter used as a VBC. This DC DPS consists of three subsystems: 1) a source converter comprising a DC power source and a simple $L_S - C_S$ filter, 2) a pulsed power load, 3) a VBC. In this configuration, a VBC has been used to damp the DC bus voltage transients or instabilities.

The detailed schematic of the bi-directional converter with a storage inductor, is shown in Fig. 2. It includes a filter capacitor C_F, a storage inductor L_{ST}, and four power switches $Q_1 \sim Q_4$. The current I_S is the source current including the disturbance current and the current I_C is the filter capacitor current. The voltage V_C is the DC bus voltage and the current I_{LST} is the storage inductor current. Also, the current γ is the transiently injected current into the DC bus from the storage inductor, in order to compensate for the finite impedance of the DC bus. Also, the injection current γ can be expressed as

$$\gamma = \begin{cases} +I_{LST} & \text{for } Q_1, Q_2 = on \\ -I_{LST} & \text{for } Q_3, Q_4 = on \end{cases} \quad (1)$$

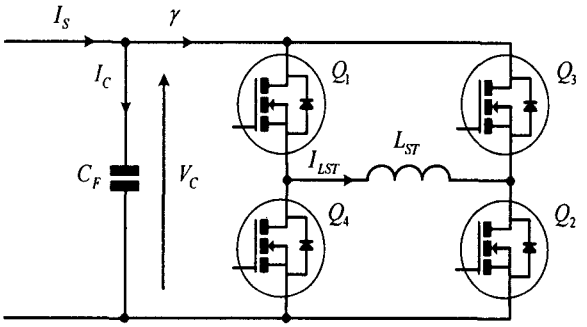

Fig. 2 A VBC with inductive storage

In Fig. 2, it assumes that the storage inductor has a smooth DC current. The filter capacitor C_F is used to reduce switching current ripples, which are caused by the conduction of a diagonal pair of switches (Q_1, Q_2) or (Q_3, Q_4).

In Fig. 1 and 2, if the pulsed power load is activated, the filter capacitor current I_C will be negative, due to the drop of the DC bus voltage. The bi-directional converter will then recognize this change and adjust the duty ratio accordingly, to facilitate the net flow of current back to the DC bus from the storage inductor. That is to say, when switches (Q_3, Q_4) are turned on, the energy of the inductive storage decreases and the DC bus voltage increases. Conversely, if the pulsed power load is deactivated, the filter capacitor current I_C will be positive because of the rise of the DC bus voltage. In order to adjust to this new condition, the bi-directional converter acknowledges the rise in the DC bus voltage and draws current to charge up the inductive storage, storing the

excess energy to release when required. Namely, when switches (Q_1, Q_2) are turned on, the energy of the inductive storage is increases and then the DC bus voltage is decreases. Therefore, the converter regulates the energy flow through the storage inductor by means of the proper switching action, and the switching action is dependant on the bus status. The energy stored in the inductor L_{ST} depends on the the square of the current flowing through it. Thus, the DC bus voltage may be stabilised through the VBC with inductive storage.

In order to look into the dynamics of the converter and the performance of the controller, the typical system parameters have to be used. In all-electric aircraft, because the high voltage DC aircraft power system (e.g., 270 Vdc or HVDC) is becoming a performance benchmark in advanced aircraft applications [7], the DC input supply voltage V_S was chosen at 270 V. Also, in an aircraft system, a synchronous machine is generally used as a generator. This machine, directly coupled to the engine shaft, provides the excitation. The output voltage is controlled by modulating the excitation of the synchronous machine, which is a fairly slow process, usually with a bandwidth of less than 10 Hz. The 400 Hz three-phase output of the generator is rectified with a full wave rectifier followed by a second-order input filter. Thus, the corner frequency of around 1 kHz for this filter was chosen, providing ample attenuation of the low-frequency ripple of the rectifier. The input filter components L_S=400 μH and C_S=50 μF was chosen. There are two important characteristics of this arrangement. Firstly, the rectifier blocks reverse current flow into the generator. Secondly, the impedance and the corner frequency of the input filter dominate the transients on the DC bus.

In this study, a step-up (boost) converter and a resistor are separately used as a short pulsed load. The step-up converter appears as a constant power load because it is tightly regulated. Both short pulsed power loads separately draw 20 A from the DC bus in the steady state. These loads are activated and deactivated at 90 Hz with a 50% duty ratio.

Furthermore, in our particular application, a short pulsed power load is rated at 10 J. Thus, the energy storage capability of the inductor is also 10 J. The average current of the load is 20 A, resulting in value of the inductor L_{ST} =50 mH. The switching frequency of the VBC was chosen to be 100 kHz, well within the capabilities of all power MOSFETs. The value of 10 μF for the filter capacitor C_F is calculated, to limit the resulting voltage ripple to around 1 % nominal voltage, i.e. 2.7 V.

3. Constant Frequency Hysteresis Control

In Fig. 3, the hysteresis control (in effect a type of SMC) has implemented attempts to respond instantaneously to voltage variations while keeping the switching frequency within the prescribed limit. Only the inductor charge and discharge modes are utilised. The switch states are determined by a comparator, which keeps the AC component of the bus voltage within the limits $v_{ac}^{*} \pm (\beta/2)$, β being the hysteresis bandwidth and v_{ac}^{*} being the desired bus voltage variation, δ is a instantaneous bus voltage error $(v_{ac} - v_{ac}^{*})$.

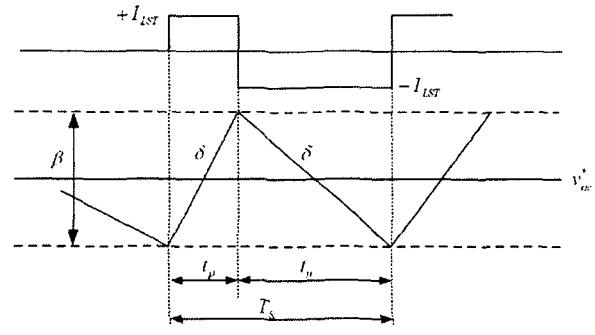

Fig. 3 Simplified waveforms for hysteresis control

In Fig. 2 and Fig. 3, the filter capacitor current I_C can be written as follows

$$I_C = C_F \frac{dV_C}{dt} \tag{2}$$

$$\therefore I_C = I_S - I_{LST} = C_F \frac{\Delta V_C}{\Delta t} = C_F \frac{v_{ac}}{\Delta t} \tag{2a}$$

For Mode 1, where the converter draws current from the bus, the switching time t_p is

$$I_S - I_{LST} = C_F \frac{\beta}{t_p} \tag{3}$$

$$\therefore t_p = \frac{\beta C_F}{I_{LST}(1 - I_n)} \tag{3a}$$

where $I_n = I_S / I_{LST}$.

Similarly, for Mode 2 and converter sinking current from the bus, the switching time t_n is

$$I_S + I_{LST} = C_F \frac{\beta}{t_n} \tag{4}$$

$$\therefore t_n = \frac{\beta C_F}{I_{LST}(1 + I_n)} \tag{4a}$$

Thus, the switching period can be then calculated as

$$T_S = \frac{1}{f_s} = t_p + t_n = \frac{2\beta C_F}{I_{LST}(1-I_n^2)} \quad (5)$$

In equation (5), if I_n varies and β is constant, a variable switching frequency is produced. However, if the hysteresis band β varies in dependence of I_n, a constant switching frequency can be obtained from equation (5). Namely, the modulation law for the PLL (Phase-Locked Loop) keeping the switching frequency constant can be derived from equation (5).

$$\beta = \frac{I_{LST}}{2f_s^* C_F}(1-I_n^2)$$

$$\text{or } f_s^* = \frac{I_{LST}}{2\beta f_s^* C_F}(1-I_n^2) \quad (6)$$

where f_s^* is the desired switching frequency.

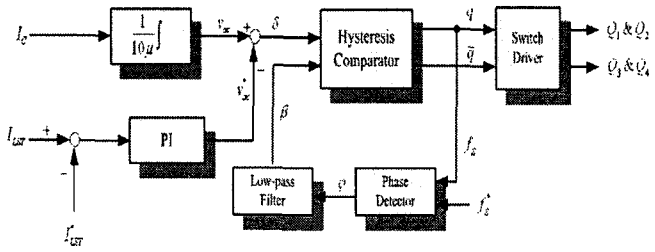

Fig. 4 Implementation of constant frequency hysteresis control

The implementation of the proposed controller is shown in the block diagram in Fig. 4. The hysteresis controller will keep the AC component of the bus voltage v_{ac} down to zero (as much as the storage current I_{LST} allows this) and will vary the hysteresis bandwidth in response to bus disturbances in order to limit the ensuing switching frequency variations. A phase detector compares the actual and the desired switching frequency. The output of the detector is filtered to produce a smooth value for the hysteresis bandwidth. A first-order filter was chosen for the purpose, with a corner frequency a decade below the targeted 100 kHz switching frequency. This somewhat conservative choice can be explained by the need for smooth signal for β.

4. Stability for the Proposed Hysteresis Controller

In Fig. 4, the transfer function of the first order filter is described with

$$TF\phi = \frac{d\beta}{d\phi} = \frac{k_f}{(s/\omega_c)+1} = \frac{k_f\omega_c}{s+\omega_c} \quad (7)$$

where k_f is a constant and w_c is a corner frequency of the filter.

The transfer function of the implemented phase detector can be approximated with

$$TF_{PHD} = \frac{d\psi}{df_s} = -\frac{2\pi}{s} \quad (8)$$

The hysteresis comparator is assumed not to introduce any dynamics or delays. From equations (5) and (6), its transfer function can be described as a DC gain only

$$TF_{HYS} = \frac{df_s}{d\beta} = -\frac{I_{LST}}{2\beta^2 C}(1-I_n^2) \quad (9)$$

By making use of equations from (5) to (9), the loop transfer function for frequency control is then

$$TF_{CLF} = \frac{4\pi C_F}{I_{LST}} \frac{f_s^{*2}}{(1-I_n^2)} \frac{k_f\omega_c}{s^2+\omega_c s} \quad (10)$$

$$= 2\pi \frac{k_f\omega_c}{s^2+\omega_c s} \frac{f_s^*}{\beta} \quad (10a)$$

In equation (10), the loop TF_{CLF} gain varies considerably with I_n. When I_n is very large, loop gain value approaches unity. On the contrary, for small value of I_n near zero the loop gain decreases. The loop gain TF_{CLF} of the equation (10a), also, varies appreciably with the hysteresis bandwidth β. Thus, the large variations of TF_{CLF} gain due to β or I_n may result in instability. To avoid instability, it is necessary to set the condition of I_n and the limit of the bandwidth β. From equation (6), the extremum values for β needed to keep the frequency constant can be calculated. For desired switching frequency and nominal storage current

$$\beta_{\min} < \beta < \beta_{\max} \quad (11)$$
$$\Rightarrow 0 < \beta < 10 \text{ for } 0 < I_S < I_{LST}$$

where f_s^*=100 kHz, C_F = 50 μF, and $0 < I_S < 20$.

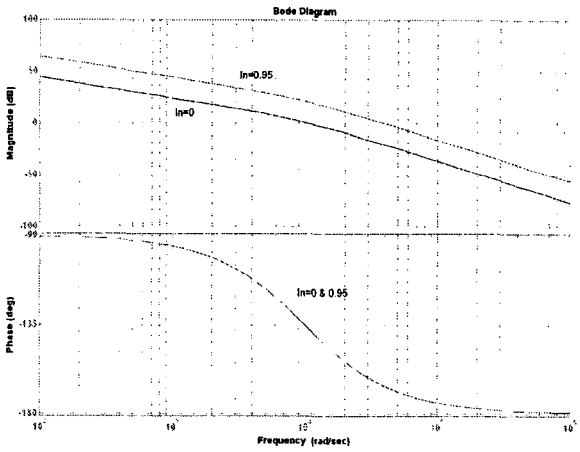

Fig. 5 Bode diagram of equation (10)

In Fig. 5, the asymptotic bode diagram for maximum and minimum diagram, corresponding to the choice adopted for the controller, are shown. The used parameters were:

ω_c=10 kHz, f_s^*=100 kHz, I_{LST} = 20 A, I_{nmin}=0, I_{nmax} =0.95, $k=0.2$, $L_{ST}=50$ mH, and C_F = 50 μF,. Therefore, the transfer function in equation (10) resulta in a phase margin of 43 degree for $I_n=0$ and 15 degree for $I_n=0.95$.

5. PI Controller for Inductor Current Control

A second loop is needed to keep the storage current I_{LST} close to the desired level of 20 A ($I_{LST}^*=20$ A). The reference input v_{ac}^* to the hysteresis comparator is modified by the error signal between the desired and the actual storage current. A proportional-integral compensator was used in this loop.

$$v_{ac}^* = k_p(I_{LST}-I_{LST}^*)+k_i\int(I_{LST}-I_{LST}^*)dt \quad (12)$$

From equation (11), the maximum value of β is 10. This means that the maximum current deviation is around 5 A. Since our target error is approximately 2A (10% of steady-state), the resulting proportionate gain should be 2. The required integral gain is to minimise any steady-state errors and compensate for the conduction losses in the power circuit. It therefore needs to be very low and in our simulation was set at 0.001.

6. Simulation results

To investigate the behaviour of the proposed controllers in a DC distributed power system with a VBC, the worst-case scenarios are simulated here. A step-up (boost) converter and a resistor are separately used as a short pulsed load. These are drawn 20 A from the DC bus in the steady state and are also activated and deactivated at 90 Hz with a 50% duty ratio. This means the case when the bus is transiently loaded from 0 % to 100 %.

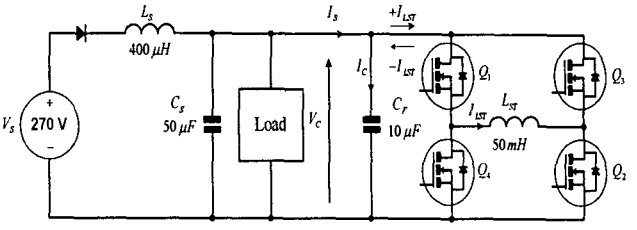

L_S and C_S are observed. The deactivation of the resistive load results in the bus voltage (329 V), which is considerably higher than the nominal voltage (270 V).

The simulation results when the step-up converter is connected as a pulsed power load are shown in Fig. 7(b). In Fig. 7(b), the voltage variations on the bus voltage without VBC are between 241 V and 315 V. When the load is activated, the large oscillations of 600 Hz, due to the interaction between the input filter and the filter of the boost converter, can also be seen. Also, as the load is deactivated, the peak voltage (315 V) is monitored and the voltage (315 V), higher than the nominal voltage (270 V), is observed.

As a result, the severe transients on the voltage bus, which are caused by short pulsed loads, result in a distributed power system. In fact, the resulting transients will heavily affect. the normal operation of other loads and may result in instability in a DPS.

6.1 System Simulation Results with VBC

In this section, two types of controller, the sliding mode controller and the constant frequency hysteresis controller, have been simulated and compared. The sliding mode controller, compared with the proposed hysteresis controller, was described fully in [17].

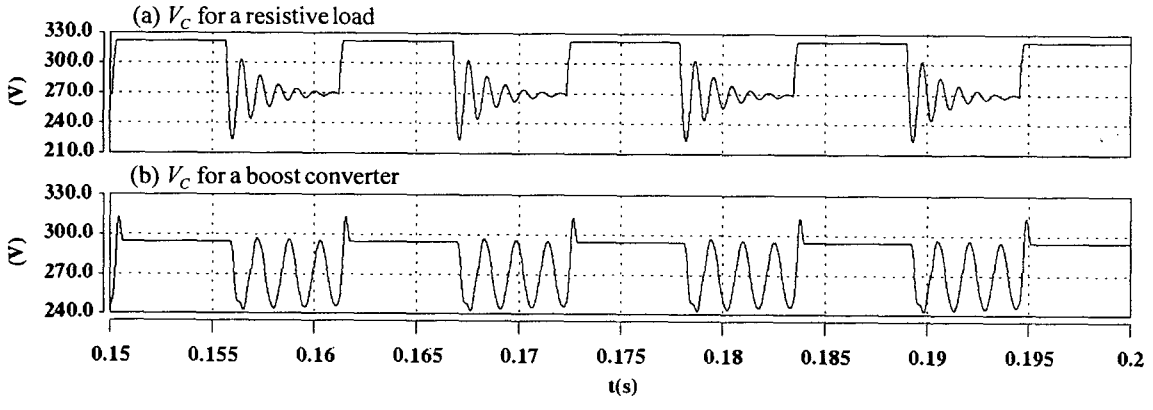

Fig. 7 Simulation Results for a DPS without a VBC

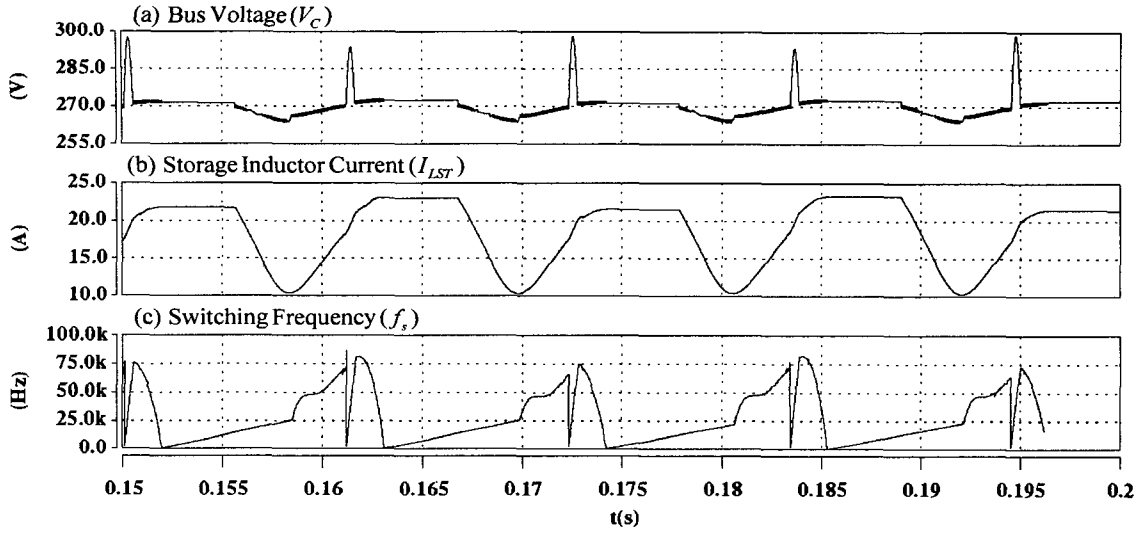

Fig. 8 Simulation results for sliding mode control

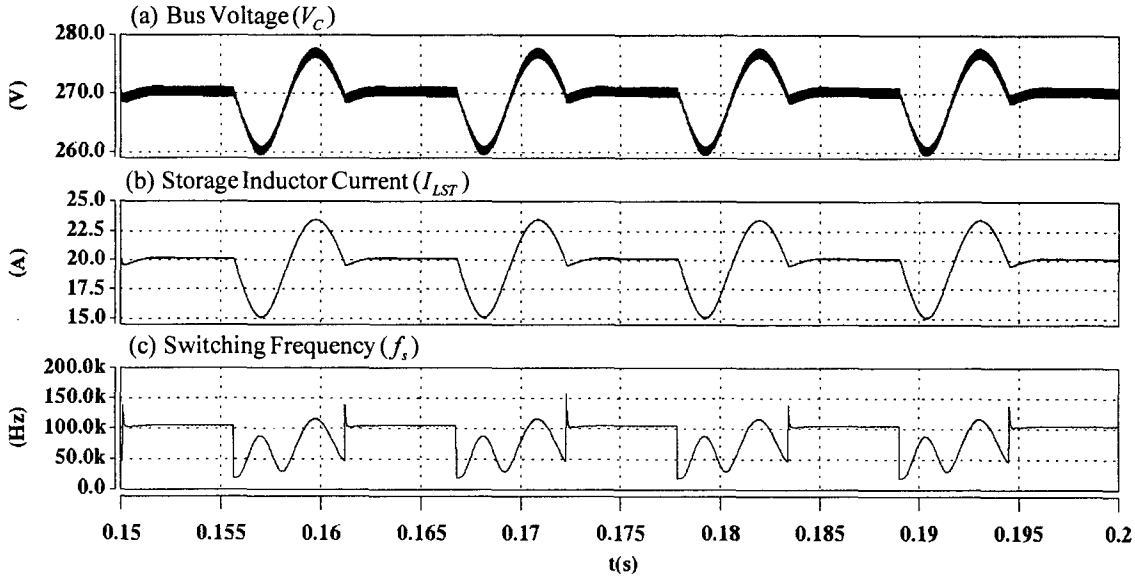

Fig. 9 Simulation results for constant frequency hysteresis control

6.1.1 Simulation Results for a Resistive Load

The simulation results for sliding mode control are shown in Fig. 8. The bus voltage variations (Fig. 8(a)) are considerably smaller and better damped. The bus voltage excurses between 263 V and 298 V. The average value of the storage inductor current (Fig. 2-8(b)) is shown below at 20 A, and the variations are also large. The waveform is obviously a little irregular, which is attributed to the discrete nature of the controller operation. The switching frequency

(Fig. 8(c)) rises to just below 90kHz when the load is deactivated, in order to absorb the energy stored in the filter inductor. Also, the controller generates a very short burst at the load switching instances, limiting the bus voltage transition to 30V.

The simulation results for constant frequency hysteresis control are shown in Fig. 9. The simulation indicates that the overall resulting bus voltage variations (Fig. 9(a)) are the lower than they are with sliding mode control. The voltage variations between 259 V and 279 V occur at load turn-on, as the available storage current cannot fully compensate for the larger disturbance current. For the duration of this instant, the VBC sources the maximum available current to the bus, and in Fig. 9(c) the switching frequency recovers slowly toward its desired switching frequency. Also, during the load turn-off, the switching frequency (Fig. 2-17(c)) is 100 kHz. The average commutation frequency is 98 kHz (Fig. 9(c)), momentarily reaching 150 kHz during load turn on.

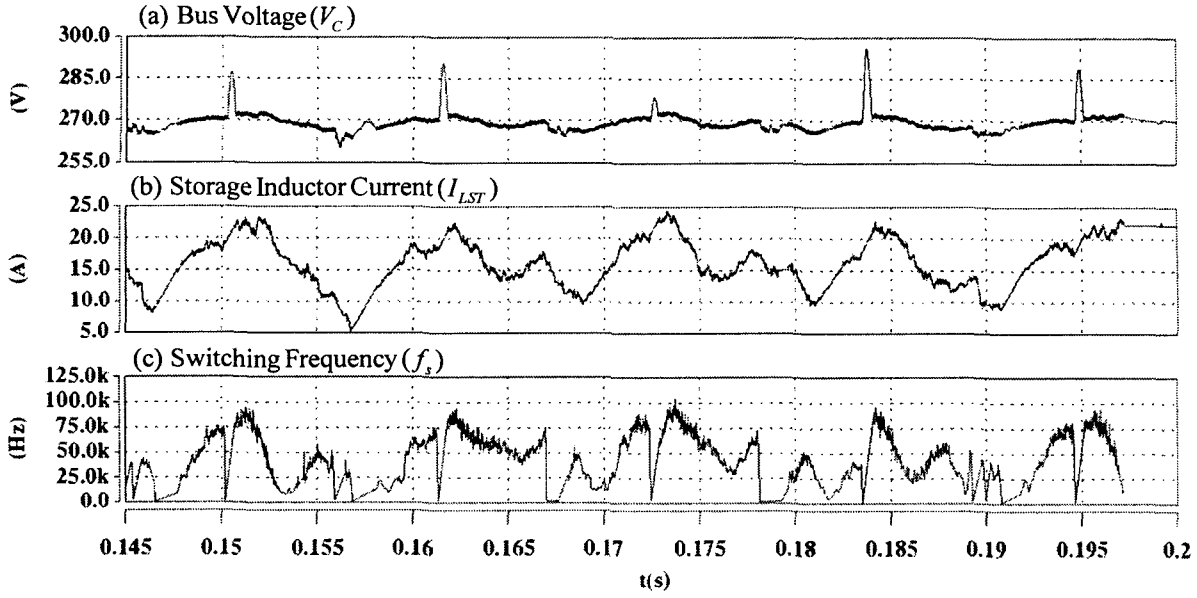

Fig. 10 Simulation results for a sliding mode control

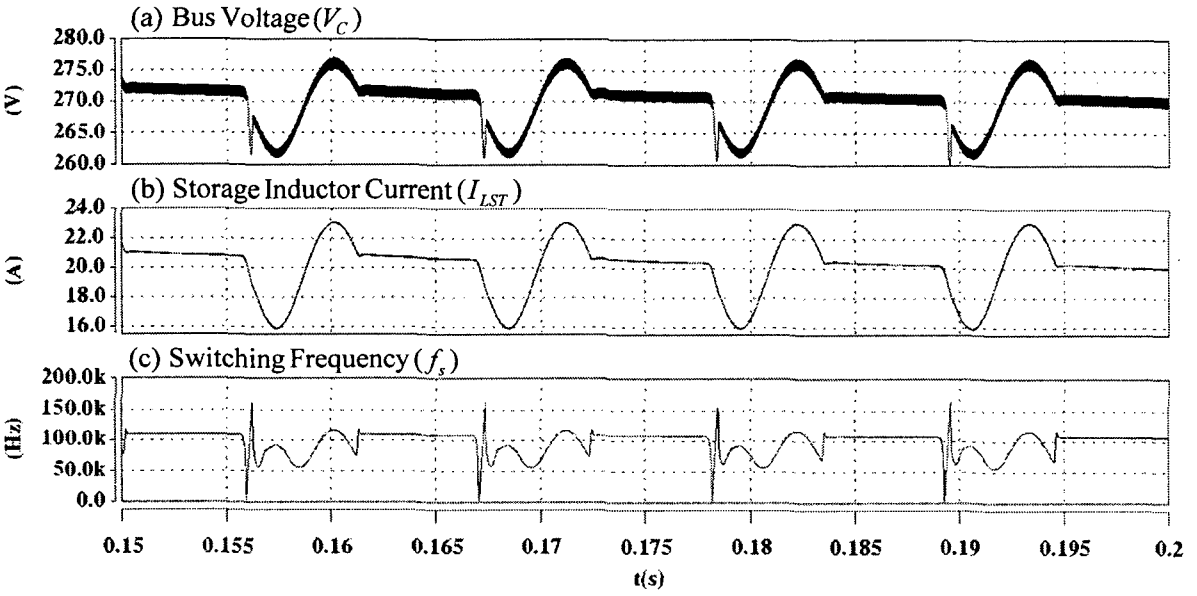

Fig. 11 Simulation results for constant frequency hysteresis control

The average storage inductor current (Fig. 2-17(b)) is slightly higher than 20 A, experiencing transitions of +3.5/-5 A. The large deviations occur after load turn-off and are explained by the need to withdraw current from the filter inductor

6.1.2 Simulation Results for a Boost Converter Load

The simulation results for sliding mode control are shown in Fig. 10. The bus voltage variations (Fig. 10(a)) are considerably smaller and better damped than they are without the VBC. The bus voltage variations are between 260 V and 296 V. The average value of the storage inductor current (Fig. 10(b)) is shown below at 20 A, but the variations are very large (5 A ~ 24 A). The waveform is obviously irregular which is also attributed to the variable switching frequency. The switching frequency (Fig. 2-10(c)) instantly reaches 97 kHz when the load is deactivated, in order to absorb the energy stored in the filter inductor. Also, the controller generates a very short burst at the load switching instances, limiting the bus voltage transition to the maximum 30 V.

The simulation results for constant frequency hysteresis control are shown in Fig. 11. In Fig. 11(a), the bus voltage variations are certainly smaller than those of

sliding mode control. The large excursions between 260 V to 276 V occur at load turn-on, as the available storage current cannot fully compensate for the larger disturbance current. For the duration of this instant, the VBC sources the maximum available current to the bus and the switch configuration remains unchanged. This is demonstrated by a zero switching frequency (Fig. 11(c)). At load turn-off, the bus voltage recovers slowly toward its steady-state bus voltage. The average storage inductor current (Fig. 11(b)) is slightly higher than 20 A, experiencing transitions of +3/-4 A. The average commutation frequency is 98 kHz (Fig. 11(c), momentarily reaching 150 kHz during load turn on. This is well within the capabilities of advanced low on-state resistance MOSFETs.

7. Conclusion

The voltage bus conditioner (VBC) with inductive storage, as described in this paper, utilises all of the stored energy, unlike its counterpart with capacitive storage. In addition, two types of hysteresis control have been compared. The simulated sliding mode controller with side bands resulted in good performance. This type of controller benefits from robust convergence and is devoid of chattering in steady-state, a problem common to most sliding-mode controllers. However, the switching frequency varies considerably with load variation, which results in the harmonic ripple of the storage inductor current and irregular converter operation. The constant frequency hysteresis control resulted in the best performance. The bus voltage excusions are very well damped. The resulting transients at load turn-on are slightly, but noticeably smaller. Therefore, the proposed constant frequency hysteresis control results in the shortest and the smallest variations.

Although the system described here has, within its scope, an aerospace application, the general principles and conclusions that can be drawn from the performance of the controllers are clearly applicable to other systems, where critical equipment needs to be protected from bus voltage variations in a dynamic and noisy environment.

참 고 문 헌

[1] C. C. Heath, "The Market for Distributed Power System", Applied Power Electronics Conference and Exposition 1991, APEC'91, Conference Proceedings 1991, 6th Annual IEEE, Mar. 1991, Page(s) 225-229.

[2] W. A. Tabisz, M. M. Jovanovic, F. C. Lee, "Present and Future of Distributed Power Systems", Applied Power Electronics Conference and Exposition 1992, APEC'92, Conference Proceedings 1992, 7th Annual IEEE, Feb. 1991, Page(s) 11-18.

[3] Scott Fish, Eric Redding, "Prime Power and Pulsed Energy Storage for EM Gun Equipped Tank Combat Missions", IEEE Transactions on Magnetics, Vol. 33, No. 1, Jan 1997, Page(s) 642-646.

[4] Richard M. Traci, Robert Acebal, "Integrated Thermal Management of a Hybrid Electrical Vehicle", IEEE Transactions on Magnetics, Vol. 35, No 1, Jan 1999, Page(s) 479-483.

[5] Thomas L. Baldwin, Shani A. Lewis, "Distribution Load Flow Methods for Shipboard Power Systmes", IEEE Transactions on Industry Applications, Vol. 40, No. 5, Sep/Oct 2004, Page(s) 1183-1190.

[6] R. I. Jones,"The More Electric Aircraft: The Past and The Future ?", Electrical Machines and Systems for the More Electric Aircraft.(Ref. No. 1999/180), IEE Colloquium on, 1999, Page(s) 4/1-4/4.

[7] D. Segret, W. W. Cloud, "Evolution and Development of High Voltage (270 Volt) DC Aircraft Electric Systems in the United States", SAE Transactionon Journal of Aerospace, Vol. 90, 1981, Page(s) 51-63.

[8] L. J. Feiner, "Power-by-wire Aircraft secondary Power System", Proc. IEEE 12th Digital Avionics Systems Conf., FortWorth, Oct1994. Page(s) 439-444.

[9] Jie Chang, Anhua Wang, "New VF-Power System Architecture and Evaluation for Future Aircraft", IEEE Transaction on Aerospace and Electronic Systems, Vol. 42, No. 2, Apr 2006, Page(s) 527-539.

[10] M. Alfayyoumi, A. H. Nayfeh, D. Borojevic, "Input Filter Interactions in DC-DC Switching Regulators", IEEE Power Electronics Specialist Conference 1999, PESC' 99, Vol. 2, Page(s) 152-159.

[11] R. L. Steigerwald, G. W. Ludwig, R. Kollman, "Investigation of Power Distribution Architecture for Distributed Avionics Loads", Power Electronics Specialists Conference 1995, PESC'95, 26thAnnual IEEE, Vol.1, Jun1995, Page(s)231-237.

[12] S. A. Bock, J. R. Pinheiro, H. Grundling, H.L. Hey, H. Pinheiro, "Existence and Stability of Sliding Modes in Bi-directional DC-DC converters", Power Electronics Specialists Conference, 2001. PESC. 2001 IEEE 32nd Annual, Vol. 3, Jun 2001, Page(s): 1277-1282.

[13] Torrey, D A., Al-Zamel, "Single-Phase Active Power Filters for Multiple Nonlinear Loads", Power Electronics, IEEE Transactions on, Vol. 10, Issue. 3, May 1995, Page(s) 263-272.

[14] E. J. P Mascarenhas, "Hysteresis Control of a Continuous Boost Regulator", Stattic Power Conversion, IEE Colloquium on, Nov 1992, Page(s) 7/1-7/4.

[15] Luigi Malesani, Paolo Mattavelli, Paolo Tomasin,

"High-Performance Hysteresis Modulation Technique for Active Filters", IEEE Transactions on Power Electronics, Vol. 12, Issue:.5, Sept. 1997, Page(s) 876-884.

[16] G. H. Bode, D. G. Homes, "Load Independent Hysteresis Current Control of a Three Level Single Phase Inverter with Constant Switching Frequency", Power Electronics Specialists Conference, 2001. PESC. 2001 IEEE 32nd Annual, Vol. 1, Jun 2001, Page(s) 14-19.

[17] Jae Du La, Yong Geun Lee, "The Comparison of Two Control Algorithm for a Voltage Bus Conditioner in a DC Power Distribution System", The Transactions of the KIEE: P, Vol. 55, No. 1, Mar 2006, Page(s) 47-53.

저 자 소 개

나 재 두 (羅 在 斗)

1970년 10월 10일생. 1994년 인천대학교 전기공학과 졸업. 1996년 인하대학교 전기공학 졸업(석사). 2003.8. G&W Tech -nologies, 선임연구원. 2003.9 - 현재, 영국 The University of Birmingham, EECE, 박사과정.

Tel : +44-121-414-3150

E-mail : jxl399@bham.ac.uk